JOURNAL OF VIROLOGY, Nov. 1984, p. 638–649
0022-538X/84/110638-12$02.00/0

Vol. 52, No. 2

Structural Organization and Polypeptide Composition of the Avian Adenovirus Core

PENG LI,† ALAN J. D. BELLETT,* AND CHRISTOPHER R. PARISH

Department of Microbiology, John Curtin School of Medical Research, Australian National University, Canberra, A.C.T. 2601, Australia

Received 19 March 1984/Accepted 31 July 1984

CELO virus (fowl adenovirus 1) contained three core polypeptides of molecular weights 20,000, 12,000, and 9,500. The core was similar to that of human adenoviruses, with some evidence of compact subcore domains. Micrococcal nuclease digestion of CELO virus cores produced a smear of DNA fragments of gradually decreasing size, with no nucleosome subunit or repeat pattern. Moreover, when digested cores were analyzed without protease treatment, there was again no evidence of a nucleosome substructure; neither DNA fragments nor core proteins entered a 4% polyacrylamide gel. The organization of the core is thus quite unlike that of chromatin. Restriction endonuclease analysis of the DNA from digested cores showed that the right end was on the outside of the core. We suggest that adenovirus DNA is condensed into the core by cross-linking and neutralization by the core proteins, beginning with the packaging sequence at the center of the core and ending with the right end of the DNA on the outside.

Adenoviruses contain an internal core that consists of the viral DNA and the virus-coded, basic core proteins. In human adenovirus, there are two prominent arginine-rich core proteins, the major core protein (polypeptide VII) and the minor core protein (polypeptide V). Of the two, the major core protein is more tightly associated with the viral DNA (4, 14, 15). A third virion polypeptide, designated μ, which is very small and very rich in arginine, may also be associated with the viral DNA (25). The adenovirus terminal protein (43, 44) is covalently linked to the 5′ ends of the viral genome.

The structure of the adenovirus core has been investigated by electron microscopy, and several different morphological structures have been proposed. Brown et al. (4) proposed that the core was organized into 12 morphological subunits, each under a vertex of the capsid. However, Nermut (38, 39) suggested that the viral DNA was wrapped around a helical filament composed of the major core protein, and that the resulting nucleoprotein was packed into six rodlike elements.

Since eucaryotic chromatin was shown to consist of a repeating nucleosome structure, a number of similar models for the adenovirus core have been proposed. Using micrococcal nuclease as a probe, Corden et al. (5) reported that the adenovirus core had a chromatin-like structure consisting of repeating subunits of 200 base pairs (bp) of DNA and core proteins. Subsequent investigators failed to reproduce the nucleosome repeat pattern in the virion core (37, 54, 57). Despite this, another chromatin-like model was proposed based on a reported nuclease-resistant 150-bp nucleosomal monomer structure (37). The absence of the expected nucleosome repeat pattern was attributed to the irregular spacing of the proposed 150-bp nucleosomal monomers along the viral DNA molecule.

In this paper, we present the results of an investigation of the protein composition, morphology, and structure of the core of an avian adenovirus. Several lines of evidence suggest that the core of fowl adenovirus 1 (CELO virus) is not organized in a chromatin-like manner and has no nucleosomal substructure. An alternative model for the adenovirus core is proposed based on these results.

MATERIALS AND METHODS

Cells and viruses. The Phelps strain of CELO virus and human adenovirus 5 (Ad5) were grown and purified as previously described (31, 33, 61).

Preparation of viral cores. Purified CELO virus particles were disrupted with 10% pyridine in 5 mM Tris (pH 8.0) for 1 h at room temperature (41). The disrupted virus particles, containing 100 to 200 μg of total viral proteins in a volume of 200 μl, were loaded onto 4.5 ml of 10% sucrose in 20 mM Tris (pH 8.0)–0.2 mM EDTA with a cushion of 0.25 ml of 60% sucrose and sedimented at 42,000 rpm for 1 h at 4°C in a Beckman SW50.1 rotor. The bottom 0.4 to 0.5 ml contained the viral cores, detected by including [^{3}H]thymidine-labeled virus as a marker. In some experiments, an 11-ml 10 to 25% sucrose gradient was centrifuged in an SW41 rotor at 30,000 rpm for 125 min at 4°C (4, 41). A portion of each fraction was used to measure protein concentration (45), and another portion was used to measure ^{3}H radioactivity. Fractions containing cores were pooled and dialyzed against two changes of 1 liter of 10 mM Tris (pH 7.5) for a total of 3 to 4 h at 4°C. Sarkosyl cores were prepared by the method of Brown et al. (4).

Chicken erythrocyte nuclei, used as a positive control for eucaryotic nucleosome repeat patterns, were prepared by the method of Hörz and Zachau (24).

Enzymes and reaction conditions. Restriction endonuclease *Eco*RI was prepared by the method of Yoshimori (Ph.D. thesis, University of California, San Francisco 1971). *Hin*dIII was from Bethesda Research Laboratories Inc. *Escherichia coli* exonuclease III was from Bio-Lab. Micrococcal nuclease was from Worthington Diagnostics. Mung Bean single-strand (ss-) endonuclease was from P-L Biochemicals, Inc.

Restriction endonuclease digestion of viral DNA was done according to Maniatis et al. (34). For micrococcal nuclease digestion, the viral cores at 20 to 40 μg of DNA per ml were

* Corresponding author.
† Present address: Institute of Microbiology, Academy of Sciences, Beijing, China.

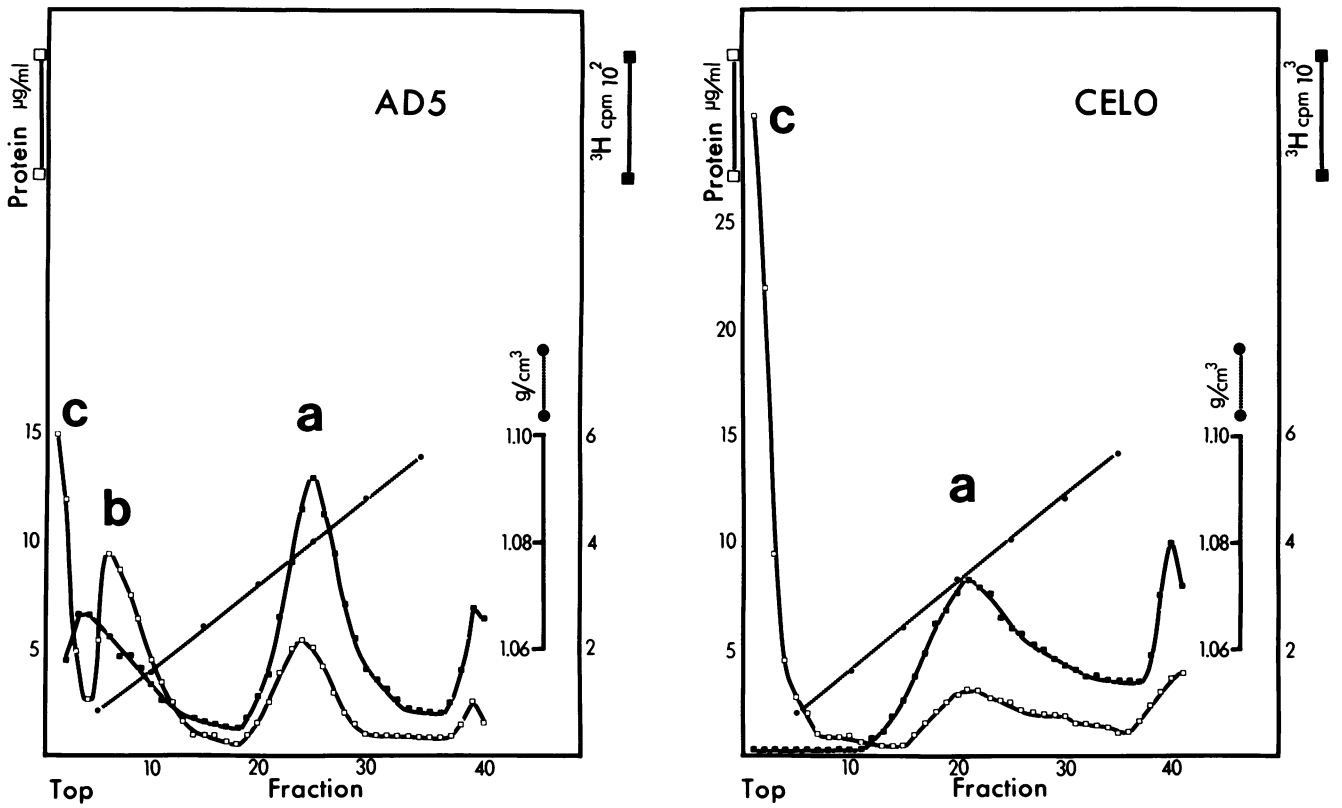

FIG. 1. Pyridine disruption of CELO virus and Ad5. [^{3}H]thymidine-labeled CELO virus and Ad5 were disrupted and analyzed by sucrose gradient sedimentation as described in the text. There was one main peak of ^{3}H radioactivity (a) in both viruses. There were two main protein peaks in CELO virus. One cosedimented with the ^{3}H radioactivity peak (a) and the other was at the top of the gradient (c). There were three protein peaks in Ad5. One cosedimented with the ^{3}H radioactivity peak (a), one was at the top of the gradient (c), and the third sedimented to fractions 6 to 8 (b). Electron microscopy (Fig. 2) and SDS-polyacrylamide gel electrophoresis (Fig. 3) demonstrated that peak a represents the viral cores, peak b represents the group of nine hexons of Ad5, and peak c represents individual viral capsomers. The gradients were monitored by measuring the refractive index of every fifth fraction.

adjusted to 10 mM Tris (pH 7.5)–1.2 mM $CaCl_2$, prewarmed to 37°C, and digested with micrococcal nuclease at 37°C. The reaction was stopped by the addition of EDTA to a final concentration of 10 mM. Samples (50 µl) of micrococcal nuclease at 1,000 U/ml in 10 mM Tris (pH 8.0) were frozen and stored at −70°C. One sample was thawed and diluted to 100 U/ml with 10 mM Tris (pH 7.5) before use. Digestion of chicken erythrocyte (RBC) nuclei by micrococcal nuclease was done at 1.0 to 1.2 mg of DNA per ml with 60 U of enzyme per ml at 37°C for 10 to 20 min. The resulting nucleosomal repeat length of DNA was found to be 200 to 210 bp when calibrated with *Hin*fI-digested pBR322 DNA fragment markers (49). This value is in agreement with that obtained by Hörz and Zachau (24).

Purified CELO virus cores were digested by exonuclease III in 5 mM Tris (pH 7.4)–5 mM NaCl–2 mM $MgCl_2$ at 750 U of enzyme per ml for 5, 10, 20, and 40 min at 37°C (a unit being defined by the manufacturer). Exonuclease III digestion of purified CELO virus DNA was done in the same way, except that the digestion was allowed to proceed for only 2, 5, 10, and 20 min. The reaction was stopped by the addition of a modified, concentrated S1 endonuclease buffer (final concentrations, 50 mM sodium acetate [pH 4.5], 30 mM NaCl, and 1 mM $ZnCl_2$), and the mixture was put on ice. After the exonuclease III digestion, all samples were warmed to 37°C and digested with 400 U of Mung Bean ss-endonuclease per ml for 10 min at 37°C (a unit being defined by the manufacturer). The digestion was stopped by the addition of EDTA to a final concentration of 10 mM.

Gel electrophoresis. Sodium dedecyl sulfate (SDS)-polyacrylamide gel electrophoresis of viral proteins was carried out according to Laemmli (30) on 10 to 20% gradient gels. Gels were stained with Coomassie brilliant blue by the formaldehyde fixation-staining method of Steck et al. (50), a procedure that effectively retains small and basic polypeptides. The silver staining method of Wray et al. (59) was employed in some experiments.

For release of DNA, purified virus particles or nuclease-digested viral cores were digested with 1 mg of protease VI (Sigma Chemical Co.) per ml and 1% SDS for 1 h. The DNA was extracted three times with phenol-chloroform-isoamyl alcohol (25:24:1) and precipitated with ethanol. After restriction endonuclease digestion, DNA fragments were separated by horizontal agarose gel electrophoresis, using a Tris-phosphate buffer system as described by Maniatis et al. (34).

Vertical polyacrylamide gel electrophoresis of DNA or nucleoproteins from virus or chicken RBC was performed by using the same Tris-phosphate buffer system. The bromophenol blue dye was run in a separate well, as this dye interferes with the DNA-ethidium bromide fluorescence and migrates on a 4 to 8% gradient polyacrylamide gel in a position between 100 and 200 bp of DNA, causing an artificial "band" by interrupting a continuous smear of DNA-ethidium bromide fluorescence. For detecting nucleo-

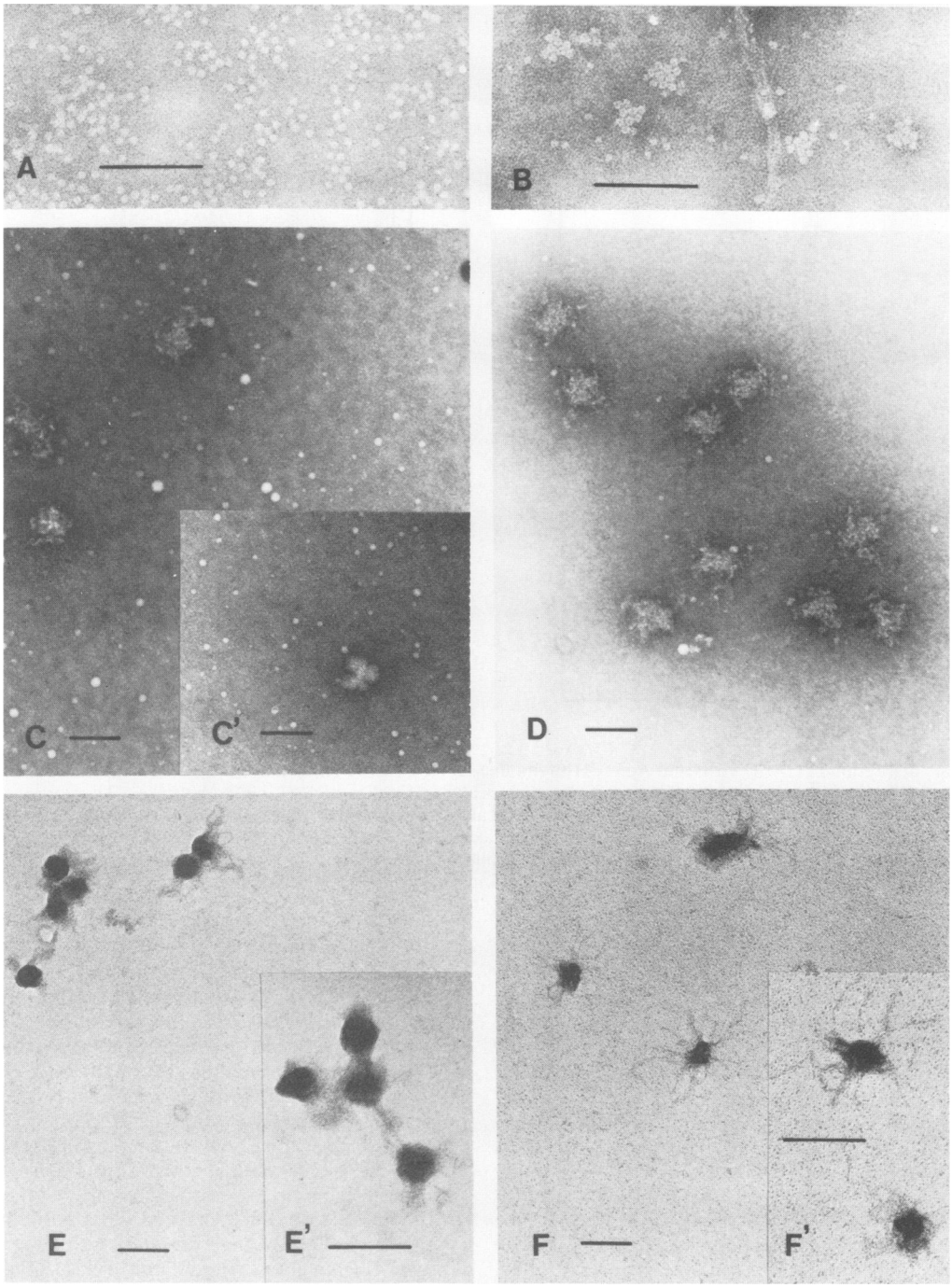

FIG. 2. Electron microscopy of pyridine-disrupted CELO virus and Ad5. The preparation of the samples is described in the text. (A) CELO virus hexons and other capsomers (fraction 1 in the CELO virus panel of Fig. 1). (B) Ad5 group of nine hexons (fraction 7 in the Ad5 panel of Fig. 1). (C and C') CELO virus cores (fraction 22 in the CELO virus panel of Fig. 1). (D) Ad5 cores (fraction 25 in the Ad5 panel of Fig. 1). Samples A to D were negatively stained with 2% sodium silicotungstate (pH 7.0). (E and E') CELO virus cores (fraction 22 in the CELO virus panel of Fig. 1). (F and F') Ad5 cores (fraction 25 in the Ad5 panel of Fig. 1). Samples E to F' were positively stained with 1% uranyl acetate (pH 4.7). The bar in each panel indicates 100 nm. The CELO virus cores appear slightly more compact than Ad5 cores.

proteins, the same gel was first stained with ethidium bromide for DNA and then stained with silver for proteins (59).

Electron microscopy. Specimen grids (400 mesh) were first covered with a Parlodion membrane formed on the surface of water and then were coated with evaporated carbon. Viral core samples were applied directly onto the grids, and the excess solution was removed with a piece of filter paper. Duplicate specimens were negatively stained with 2% silicotungstate (pH 7.0) and positively stained with 1% uranyl acetate (pH 4.7). Electron micrographs were taken with a Philips 301S electron microscope.

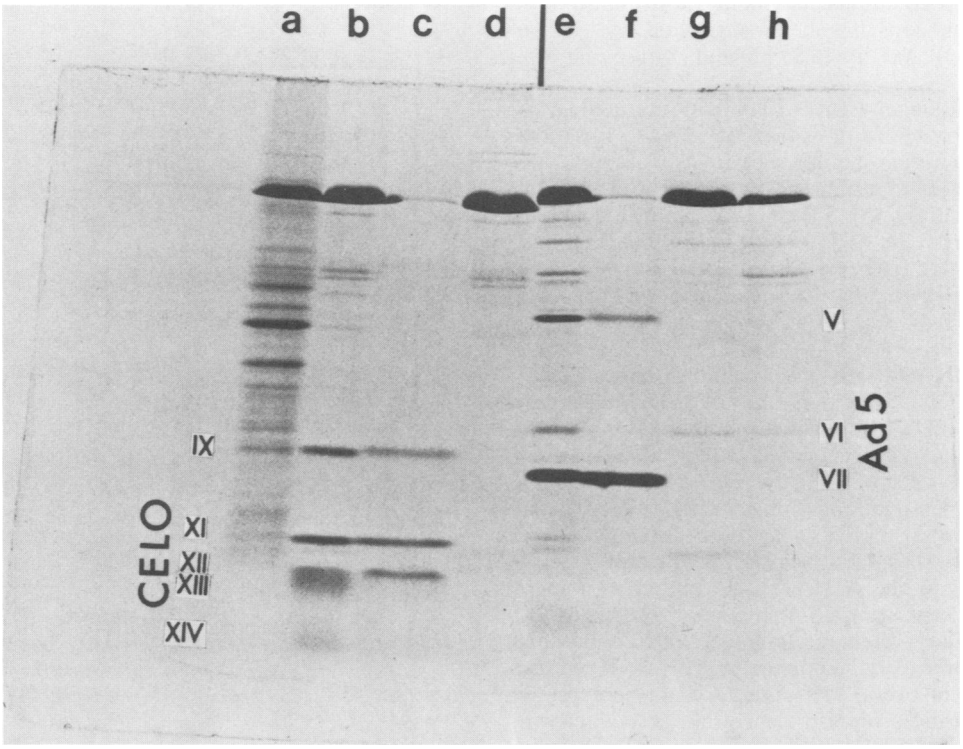

FIG. 3. Protein composition of CELO virus cores. Samples were prepared as described in the text and were analyzed by electrophoresis on a 10 to 20% gradient SDS-polyacrylamide gel. Protein bands were visualized by Coomassie blue staining. Lanes: a, the "light band" from CELO virus-infected CEK cells; b, CELO virions; c, CELO virus cores (fractions 18 to 30 in the CELO virus panel of Fig. 1); d, CELO virus capsomers (fractions 1 to 3 in the CELO virus panel of Fig. 1); e, Ad5 virions; f, Ad5 cores (fractions 21 to 30 in the Ad5 panel of Fig. 1); g, Ad5 group of nine hexons (fractions 6 to 10 in the Ad5 panel of Fig. 1); h, nonaggregated Ad5 capsomers (fractions 1 to 3 in the Ad5 panel of Fig. 1). Note that CELO virus cores contain three prominent core proteins (CELO virion polypeptides IX, XI, and XII). CELO virion polypeptide XIII is clearly not a core component; polypeptides XII and XIII migrated very close together on the gel of CELO virions.

RESULTS

Isolation of CELO virus cores by the pyridine method: a comparison with Ad5. Mild disruption of human adenovirus particles by pyridine releases two subvirion structures: "group of nine" hexons, and virus cores. The viral core released by pyridine is an "intact" structure in that it retains both of the two prominent human adenovirus core proteins (4, 41).

Figure 1 shows the sedimentation profiles of pyridine-disrupted Ad5 and CELO virus. In both viruses, there was a peak of ^3H radioactivity (Fig. 1a) which sedimented in the middle of the gradient, and a protein peak in the same fractions. This represents the viral cores (see below). The top protein peak (Fig. 1c), which represents individual viral capsomers (see below), could also be found in both viruses. However, another protein peak (Fig. 1b) in Ad5, which represents the group of nine hexons (see below), was absent in the CELO virus gradient. These results indicate that incubation with 10% pyridine can release cores from CELO virus particles, but, as reported previously for other methods of disruption (31), cannot generate CELO virus group of nine hexons.

Figure 2 shows electron micrographs of negatively stained material from the gradients shown in Fig. 1, which identify some of the morphological structures corresponding to the protein peaks. Figure 2A shows CELO virus hexons and other capsomers from fraction 1 (peak c) of the CELO virus gradient. Figure 2B is an electron micrograph of fraction 7 (peak b) of the Ad5 gradient showing group of nine hexons and some monomers. The lack of group of nine hexons in CELO virus implies that details of the assembly of the two viruses are different.

Electron micrographs in Fig. 2C to Fig. 2F′ show that peak a from the gradient of pyridine-disrupted CELO virus or Ad5 consisted of cores. When negatively stained, the CELO virus cores (Fig. 2C and C′) appeared similar to Ad5 cores (Fig. 2D), but slightly larger and more compact. Occasionally, CELO virus cores showed a very compact structure with well-defined subcore domains (Fig. 2C′). The negatively stained CELO virus cores were roughly spherical and measured ca. 80 nm in diameter. The negatively stained Ad5 cores were slightly less compact and ca. 75 to 80 nm in diameter. The sizes of the cores from both viruses were comparable to the sizes of the virions, which indicated that the cores prepared by this method were not greatly relaxed.

Slight differences between CELO virus cores and Ad5 cores were also observed by positive staining with uranyl acetate. The positively stained CELO virus cores (Fig. 2E and E′) demonstrated the existence of a compact, electron-dense body. On the other hand, positively stained Ad5 cores (Fig. 2F and F′) showed fibrous structures protruding from a less compact and less defined electron-dense body. In the positively stained cores of both viruses, a lightly stained area around the electron-dense body can be recognized. The electron-dense body may be the DNA-containing part of the core, preferentially stained under these conditions (22), and the lightly stained area may consist mainly of protein(s). The

existence of these two compartments in the structure of the human adenovirus core has been suggested by electron microscopy (4, 39) and by neutron and X-ray scattering studies (10).

Protein composition of CELO virus cores: a comparison with Ad5. The protein composition of CELO virus cores prepared by the pyridine method was investigated by SDS-polyacrylamide gel electrophoresis in comparison with that of Ad5 cores. Fractions 1 to 3 (peak c), 6 to 10 (peak b) and 21 to 30 (peak a) from the Ad5 panel of Fig. 1, and fractions 1 to 3 (peak c) and 18 to 30 (peak a) from the CELO virus panel were separately pooled, dialyzed against 5 mM Tris (pH 7.0)–0.5 mM EDTA, freeze-dried, solubilized, and analyzed by gel electrophoresis. The "light band" from CELO virus-infected CEK cells (60) was also included, since it has a greatly reduced DNA content (P. Li, A. J. D. Bellett, and C. R. Parish, J. Gen. Virol., in press) and may be a precursor capsid in CELO virus morphogenesis (60) which contains reduced amounts of CELO virus core proteins (I. Maichle-Lauppe, personal communication).

Results shown in Fig. 3 clearly demonstrate that although Ad5 cores (lane f) contained two prominent core proteins (Ad5 polypeptides V and VII), CELO virus cores (lane c) contained three. These are CELO virus polypeptides IX, XI, and XII (molecular weights, 20,000, 12,000, and 9,500, respectively) according to the nomenclature introduced elsewhere (Li et al., in press). The third CELO core protein (polypeptide XII) and a protein clearly not associated with the core (polypeptide XIII) migrated close together and formed one broad band on the polyacrylamide gel (compare lanes b and c in Fig. 3). In the CELO virus core fractions, a small amount of CELO virus hexons (31) (polypeptide II) was also present as a contaminant. The light band from CELO virus-infected CEK cells (Fig. 3, lane a) did not contain CELO virus core polypeptides XI and XII, but a small amount of CELO virus core polypeptide IX was found associated with this material. CELO virus cores prepared by the Sarkosyl method (4) contained only small amounts of polypeptide XII detectable by silver staining (59), but lacked polypeptides IX and XI (data not shown). Lane d (Fig. 3) showed that the top fractions (1 to 3) in the CELO virus panel in Fig. 1 contained most of the CELO capsid polypeptides not associated with the viral core. Lane g, the Ad5 group of nine hexons (fractions 6 to 10 in the Ad5 panel of Fig. 1), consisted of Ad5 hexons and two hexon-associated polypeptides, VI and IX, in agreement with previously published results (56).

It should be noted that CELO virion polypeptides IX, XI, and XII are prominent core proteins. They are comparable in abundance to the two prominent core proteins in human adenoviruses, and can be readily detected by Coomassie blue staining. More sensitive methods may detect more CELO virion proteins that are associated with the viral core. For instance, the CELO virus genome-linked terminal protein was identified by extensive purification followed by radioiodination (32).

Kinetics of micrococcal nuclease digestion of the CELO virus cores. [^{3}H]thymidine-labeled CELO virus was mixed with unlabeled CELO virus; viral cores were prepared by the pyridine method (see above) and digested with 1.5 U of micrococcal nuclease per ml; and the acid-insoluble radioactivity remaining was determined at intervals. Purified [^{3}H]thymidine-labeled CELO virus DNA was digested in the same way. Figure 4 shows that purified CELO virus DNA (open squares) was digested more quickly than DNA in viral cores (solid squares). Both the initial digestion rates and the

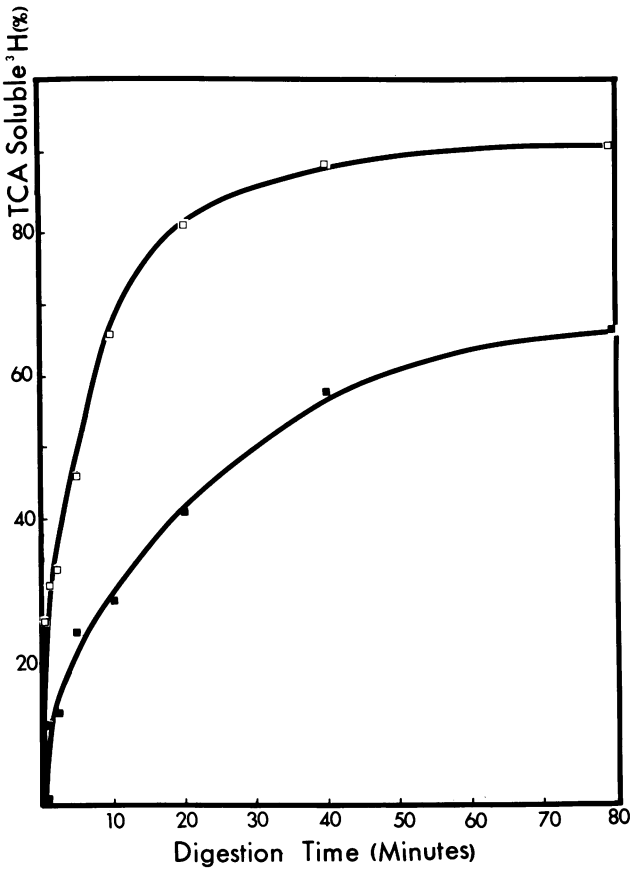

FIG. 4. Kinetics of micrococcal nuclease digestion of CELO virus cores. [^{3}H]thymidine-labeled CELO virus cores and DNA were prepared and digested with micrococcal nuclease as described in the text. The extent of digestion was measured by the ^{3}H radioactivity that was rendered acid soluble. Open squares indicate purified CELO virus DNA digested with 1.5 U of micrococcal nuclease per ml; solid squares indicate CELO virus cores digested with 1.5 U of micrococcal nuclease per ml.

portions of DNA that remained acid insoluble after extensive digestion were different. This resistance to micrococcal nuclease of the CELO virus cores is similar to that of human adenovirus cores (5, 37).

Analysis of micrococcal nuclease-digested CELO virus cores by gel electrophoresis. The two chromatin-like models for the structure of the human adenovirus core were based mainly on analysis by gel electrophoresis of the DNA fragments in micrococcal nuclease-digested cores (5, 37). The discovery by Hewish and Burgoyne (23) that nuclease digestion of eucaryotic chromatin gave rise to DNA fragments with a repeating pattern of multiples of ca. 200 bp provided a simple and reliable method for judging a chromatin-like structure. When a nucleosome repeat pattern cannot be seen but a protective effect is found, as in the case of adenovirus cores (37), the analysis of DNA alone does not give any positive answer as to whether the DNA and proteins are organized in a nucleosome-like manner. Other types of protein-DNA interactions or condensation of DNA by polyamines or other cations may also protect DNA from nuclease digestion (35). A simple method to further test whether the adenovirus core has a nucleosome-like subunit is to analyze the micrococcal nuclease-digested cores as nucleoproteins by polyacrylamide gel electrophoresis (19). A nucleosome-like structure

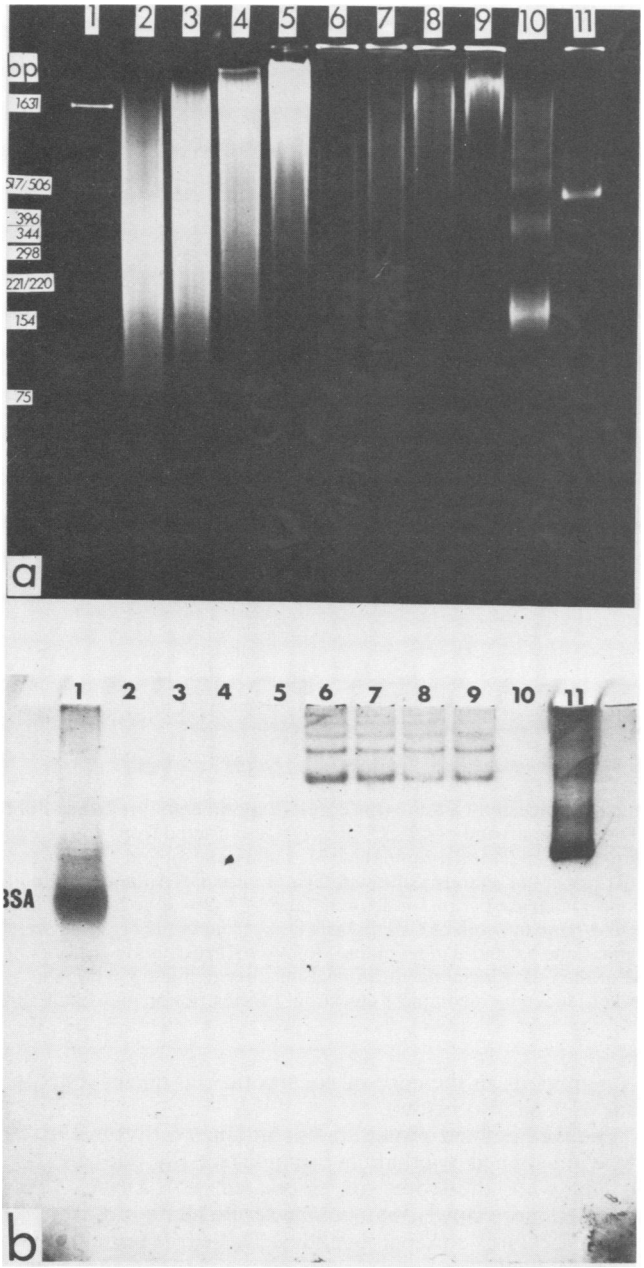

FIG. 5. Analysis of micrococcal nuclease-digested CELO virus cores. Micrococcal nuclease-digested CELO virus cores (lanes 6 to 9) and the DNAs extracted from the micrococcal nuclease-digested CELO virus cores (lanes 2 to 5) were analyzed by electrophoresis on a 4 to 8% gradient polyacrylamide gel. Lane 1, *Hin*fI-digested pBR322 DNA as size markers in base pairs (48). Lanes 2 and 6, cores digested by 1.5 U of micrococcal nuclease per ml for 20 min; lanes 3 and 7, 10 min; lanes 4 and 8, 5 min; lanes 5 and 9, 2 min. Lane 10, DNA extracted from micrococcal nuclease-digested chicken RBC nuclei. Lane 11, micrococcal nuclease-digested chicken RBC nuclei. (a) The gel stained with ethidium bromide. (b) Same gel stained with silver according to Wray et al. (59). BSA in lane 1 indicates the bovine serum albumin in the *Hin*fI-digested pBR322 DNA marker.

would enter the gel giving rise to repeated bands if there were a constant interval between units, or a sharp monomer band and broad repeat bands if the interval were variable. The same bands, in addition, should be detectable by staining for DNA and for proteins.

CELO virus cores were prepared and digested with 1.5 U of micrococcal nuclease per ml as described above. At intervals, a sample of cores was taken, adjusted to 0.01 M EDTA, and divided into two parts. Samples of set A were treated with protease VI and DNA was extracted; samples of set B were left as nucleoprotein. Both were precipitated with ethanol, pelleted in an Eppendorf centrifuge, and dissolved in 10 mM Tris (pH 8.0). Chicken RBC nuclei, used as a positive control for eucaryotic nucleosome structure, were prepared and digested with micrococcal nuclease as described above. Similarly, one-half of the micrococcal nuclease-digested chicken RBC nuclei was subjected to protease VI treatment and the DNA was extracted. The samples were analyzed by gel electrophoresis, using *Hin*fI-digested pBR322 DNA fragments as size markers. Figure 5a shows that the DNA extracted from the micrococcal nuclease-digested chicken RBC nuclei (lane 10) exhibited a typical nucleosome repeat pattern with 200 to 210-bp intervals, with a monomer DNA band of ca. 190 bp. In contrast, the DNA extracted from micrococcal nuclease-digested CELO virus cores displayed a smear in all samples. The average size of DNA decreased with increasing micrococcal nuclease digestion. After 2 min of digestion, the DNA fragments ranged from ca. 3,000 to 200 bp (Fig. 5a, lane 5). After 20 min of micrococcal digestion, when more than 40% of the DNA in the viral cores was rendered acid soluble (see Fig. 4), the protected DNA in the CELO virus core ranged from ca. 1,600 to 70 bp in size (Fig. 5a, lane 2). The DNA smear went past the 150-bp position with no "band" clearly defined, although after extensive digestion the smear seemed to have a concentrated region ranging from 500 to 150 bp in size. These digestion conditions (1.5 U of micrococcal nuclease per ml for 20 min) were more intensive than those of Mirza and Weber (37) (0.5 U of micrococcal nuclease for 10 min). Many attempts (including 80 min of digestion at 1.5 U of micrococcal nuclease per ml) to show nucleosome repeat patterns (5) or to show a 150-bp-long DNA "monomer" band (37) were unsuccessful. The *Hin*fI-digested pBR322 DNA marker (Fig. 5a, lane 1) indicated that the 4 to 8% gradient polyacrylamide gel was able to resolve DNA fragments less than 100 bp in size. The chicken RBC nuclei control always gave rise to a nucleosome repeat pattern that was not greatly influenced by the length of the digestion time. Thus, it appears that the inability to detect a nucleosome repeat pattern with the DNA from micrococcal nuclease-digested CELO virus cores, as with the DNA from human adenovirus cores (37, 54, 57), is not a technical problem. Instead, this is most likely due to the lack of a chromatin-like structure in the CELO virus core. There may be differences between avian and human adenoviruses concerning the structural organization of the cores, but the results we have obtained (Fig. 5a, lanes 2 to 5) are very similar to those published for human adenoviruses (57).

When the micrococcal nuclease-digested CELO virus cores were directly analyzed on the same gel without protease digestion and extraction of DNA, it was found that the bulk of the DNA did not enter the gel (Fig. 5a, lanes 6 to 9). As the only difference between set A samples (lanes 2 through 5) and set B samples (lanes 6 through 9) was that the latter did not receive protease digestion and phenol extraction, the core protein molecules must have held the DNA fragments together in a way that prevented entry into a 4% acrylamide gel. Ethanol precipitation itself did not seem to influence this result, as nucleoproteins of ethanol-precipitated chicken RBC nuclei were able to enter the gel. The small amount of the DNA-containing material from the micrococ-

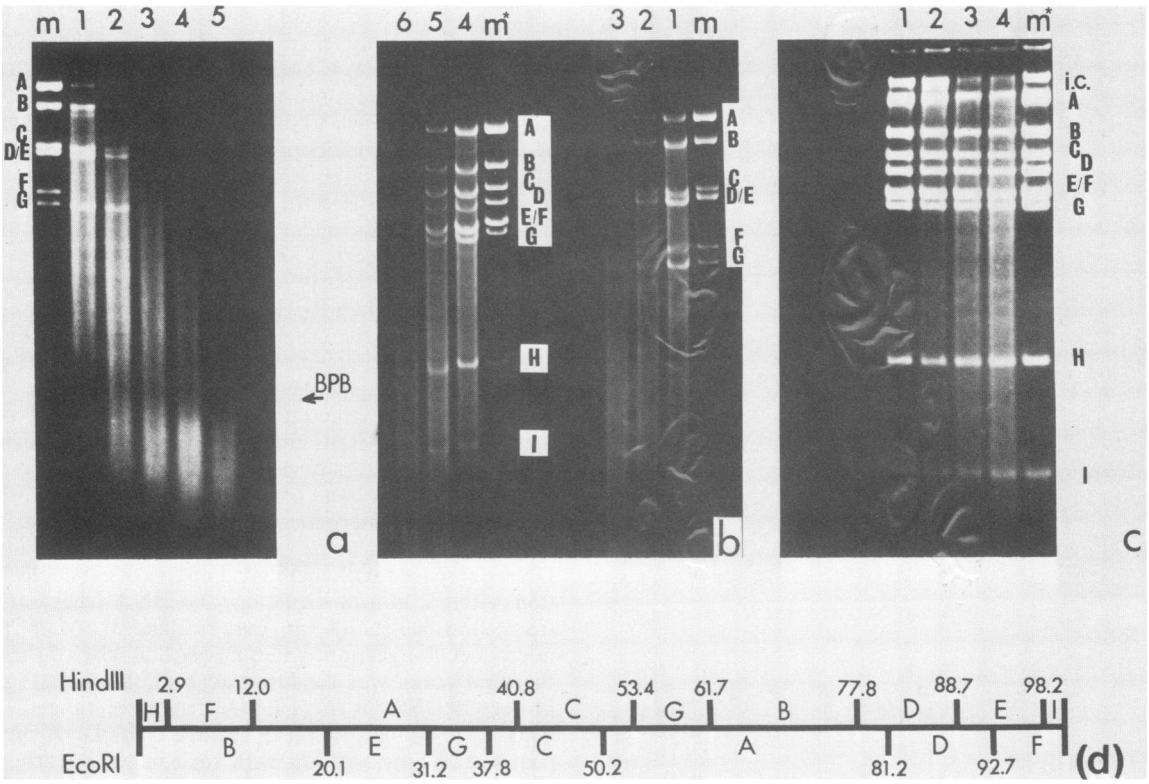

FIG. 6. Restriction endonuclease analysis of DNA from micrococcal nuclease-digested CELO virus cores. Experimental procedures are described in the text. (a) *Eco*RI restriction patterns of intact CELO virus DNA (lane m) and of CELO virus DNA extracted from viral cores that were digested with 1.5 U of micrococcal nuclease per ml for 0.5 min (lane 1), 1 min (lane 2), 2 min (lane 3), 5 min (lane 4), and 10 min (lane 5). BPB indicates the migration position of bromophenol blue dye. (b) *Eco*RI restriction patterns of intact CELO virus DNA (lane m) and of CELO virus DNA from viral cores that were digested with 1.2 U of micrococcal nuclease per ml for 0.5 min (lane 1), 1 min (lane 2), and 2 min (lane 3). Also shown are *Hin*dIII restriction patterns of intact CELO virus DNA (lane m*) and of CELO virus DNA from viral cores that were digested with 1.2 U of micrococcal nuclease per ml for 0.5 min (lane 4), 1 min (lane 5), and 2 min (lane 6). (c) *Hin*dIII restriction patterns of CELO virus DNA that was digested for 1.5 min with micrococcal nuclease at the following concentrations (units per milliliter): 0 (lane m*), 0.025 (lane 1), 0.05 (lane 2), 0.1 (lane 3), and 0.2 (lane 4). i.c. indicates a band produced by incomplete digestion. (d) Restriction map of CELO virus DNA from Denisova et al. (9).

cal nuclease-digested cores (Fig. 5a, lanes 6 to 9) that entered the gel also appeared as a broad smear. By contrast, the micrococcal nuclease-digested chicken RBC nuclei (lane 11) exhibited well-defined bands. This again suggested that the CELO virus cores did not have a chromatin-like structure.

The same gel was subsequently stained with silver according to Wray et al. (59) for protein bands (Fig. 5b). As expected, the protease-treated samples (lanes 2 to 5) and the protease-treated micrococcal nuclease-digested chicken RBC nuclei (lane 10) were not stained. The *Hin*fI-digested pBR322 DNA marker (lane 1) contained 0.3 μg of bovine serum albumin in the restriction endonuclease digestion buffer, visible in lane 1. As shown in Figure 5b, lanes 6 to 9, the micrococcal nuclease-digested CELO virus cores (without protease treatment) did not contain protein bands that corresponded to the DNA-containing material shown in the same tracks stained by ethidium bromide (Fig. 5a, lanes 6 to 9). This indicated that no nucleoprotein in the micrococcal nuclease-digested viral cores entered the polyacrylamide gel. In particular, this result argues against the proposed 150-bp nucleosome-core structure (37) in the adenovirus core. Such a structure, after micrococcal nuclease digestion but before protease digestion, would be able to enter the polyacrylamide gel. The resulting nucleoprotein bands should be detected by both DNA-specific and protein-specific stains, as is obvious in the case of eucaryotic cell nuclei (Fig. 5b, lane 11; see also below).

The well-defined protein bands in lanes 6 to 9 in Fig. 5b were not stained by ethidium bromide (see Fig. 5a, lanes 6 to 9) and were therefore not associated with DNA. These migrated more slowly than bovine serum albumin and any of the CELO virus core polypeptides. These free protein bands are most likely the hexons that contaminate the core preparation (see Fig. 3) and their oligomers, as the gel was not run under denaturing conditions.

In contrast, lane 11 in Fig. 5a and 5b clearly shows that the nucleosomes of micrococcal nuclease-digested chicken RBC nuclei (without protease treatment) entered the gel, as the same bands were detected by both ethidium bromide and by a protein-specific silver stain.

The right terminus of CELO virus DNA is on the outside of the core. Purified CELO virus particles were disrupted by pyridine, and virus cores were prepared and digested with 1.5 U of micrococcal nuclease per ml for various times. DNA was extracted, concentrated by ethanol precipitation, and further digested by *Eco*RI. The resulting DNA fragments were analyzed by electrophoresis on a 1% agarose gel. Purified CELO virus DNA was also digested with *Eco*RI and run on the same gel. The gel was stained with ethidium bromide, and the DNA bands were visualized under a UV lamp.

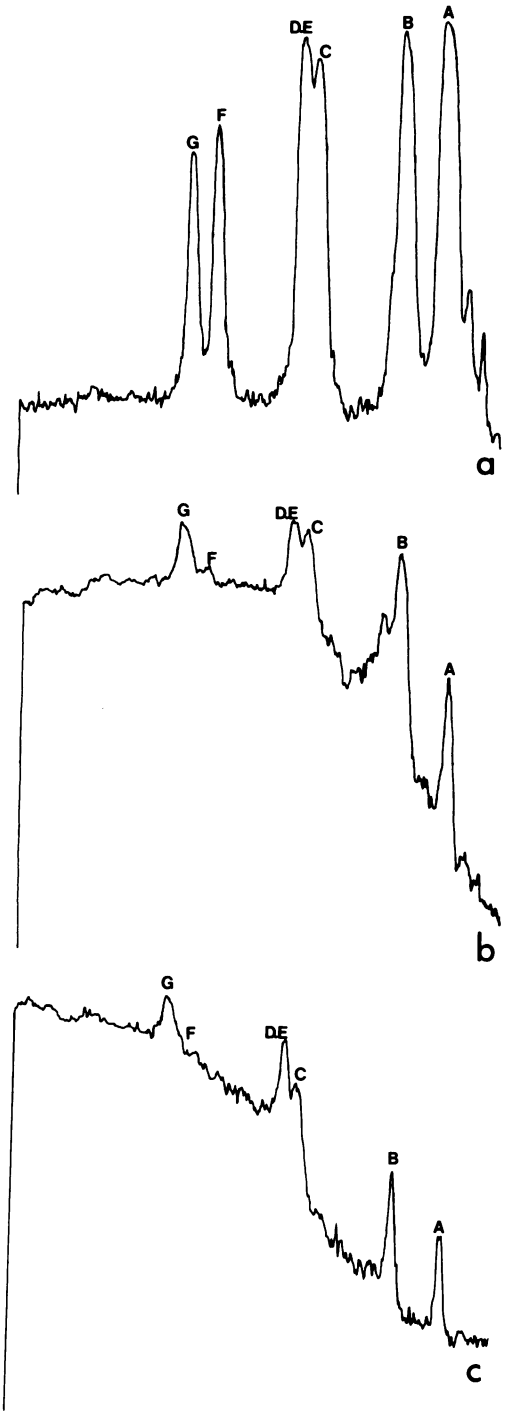

FIG. 7. Densitometer tracings of *Eco*RI restriction patterns of intact CELO virus DNA and of CELO virus DNA extracted from micrococcal nuclease-digested viral cores. The negative film of the gel shown in Fig. 6 was scanned with an LKB 2202 Ultrascan Laser Densitometer. (a) *Eco*RI restriction pattern of intact CELO virus DNA. (b and c) *Eco*RI restriction of CELO virus DNA from viral cores that were digested with 1.5 U of micrococcal nuclease per ml for 0.5 min (b) or 1 min (c). F (the right terminal) fragment was digested more quickly than other fragments (see the CELO virus DNA restriction map in Fig. 6).

The results are shown in Fig. 6a, and densitometer tracings from this gel are shown in Fig. 7. These clearly demonstrated that when the DNA was organized in the viral core, the *Eco*RI F fragment, the right terminal fragment of CELO virus DNA, was preferentially digested by micrococcal nuclease (see the CELO virus DNA restriction map in Fig. 6d). After 0.5 min of micrococcal nuclease digestion (Fig. 6a, lane 1; Fig. 7b), the *Eco*RI F fragment was virtually completely digested, whereas all other fragments were clearly recognizable and were still present after a 1-min micrococcal nuclease digestion (Fig. 6a, lane 2; Fig. 7c). In this experiment, the rate at which a particular fragment diminishes depends on two factors: the size of the fragment, and the structure-imposed accessibility of micrococcal nuclease to the fragment. The larger the fragment, the higher is the probability of a random micrococcal nuclease cut within the fragment. In an *Eco*RI digest of CELO virus DNA, the F fragment is the second smallest, so that the preferential digestion of this *Eco*RI F fragment could not be due to the size effect. Note that in Fig. 6a, the micrococcal nuclease-generated small DNA fragments were recovered as a broad smear and the bromophenol blue caused an artificial "band" at the bottom of the gel.

The *Eco*RI digestion results were reproduced many times (Fig. 6b, lanes m, 1, 2, and 3), with the right terminal (F) fragment always disappearing more quickly than other fragments. When the DNA from micrococcal nuclease-digested CELO virus cores was digested with another restriction endonuclease, *Hin*dIII, the same result was obtained. The right terminal (I) fragment was found to be more vulnerable to micrococcal nuclease digestion than other *Hin*dIII fragments (Fig. 6b). In a *Hin*dIII digest, the left terminal (H) fragment is more than 55% larger than the right terminal (I) fragment; therefore, a quicker micrococcal nuclease digestion of the H fragment would be expected because of the size effect. The quicker disappearance of the I fragment actually observed (Fig. 6b, lane 6) therefore strongly supports the conclusion that the preferential micrococcal nuclease digestion of the right terminal fragment of the CELO virus DNA resulted from the structural organization of the core.

The right-hand terminus of adenovirus DNA (including CELO virus DNA), in the conventional orientation, is the region rich in adenylate and thymidylate residues (11, 62). Earlier studies have also reported that micrococcal nuclease catalyzes preferential endohydrolysis of calf thymus DNA at A+T-rich sites (42). For a test of whether the results we have obtained were seriously influenced by this reported specificity of micrococcal nuclease, purified CELO virus DNA was digested with 0.025, 0.05, 0.1, and 0.2 U of micrococcal nuclease per ml for 1.5 min under the same conditions as the core digestions. The micrococcal neclease-digested CELO virus DNA was then analyzed by *Hin*dIII digestion. The results (Fig. 6c) showed that with increasing micrococcal nuclease digestion, the larger fragments were digested faster than the smaller fragments. This was expected from the "size effect" discussed above. When this size effect was already very obvious (Fig. 6c, lanes 3 and 4), there was no detectable preferential digestion of either terminal fragment (H or I). This control experiment further demonstrated that it is the core structure, rather than intrinsic properties of the viral DNA or of the micrococcal nuclease, that is responsible for the vulnerability of the right-hand end of the viral DNA to micrococcal nuclease digestion.

Analysis of the structure of the CELO virus core by other nucleases. Micrococcal nuclease is the most commonly used nuclease for probing the structure of chromatin and other

forms of nucleoproteins. Other nucleases with different specificities, such as DNases I and II, have also been used (16, 24). Since an appropriate exonuclease that can digest viral DNA in the cores would give independent information about the structural organization of the core, an experiment involving exonuclease III digestion followed by Mung Bean ss-endonuclease digestion of the CELO virus cores was done. *E. coli* exonuclease III catalyzes the stepwise 3′ to 5′ removal of mononucleotides from double-stranded DNA (34). With this enzyme, long single-stranded regions resulting from digestion of the double-stranded DNA termini were removed by Mung Bean ss-endonuclease, and the remaining double-stranded DNA was analyzed by restriction endonuclease digestion. Cores and CELO virus DNA that had not been exposed to exonuclease III were included in the Mung Bean ss-endonuclease digestion as controls. The samples were treated with protease VI, and the DNAs were extracted and digested with *Hin*dIII. The *Hin*dIII digests were analyzed by electrophoresis on a 1.2% agarose gel.

The results (Fig. 8) showed that digestions with exonuclease III and then Mung Bean ss-endonuclease cut the purified CELO virus DNA from both termini (lanes 1 to 5). At the left-hand side of the DNA, the order of digestion was H to F to A fragments, and on the right-hand side it was I to E to D fragments, as expected (see the restriction maps of CELO DNA in Fig. 6). Digestion of DNA in the core (Fig. 8, lanes 6 to 10) was much slower, but clearly the right terminal (I) fragment was digested more quickly than the left terminal (H) fragment. A smear below the H fragment persisted often up to 40 min of exonuclease III digestion, whereas the I fragment disappeared after 10 min of digestion. As a progressive exonuclease, exonuclease III would be expected to have an equal rate of digestion of both termini of the viral DNA in the core if both ends were equally accessible. After digestion with exonuclease III and then Mung Bean ss-endonuclease, the "trimmed" terminal fragments would no longer migrate in the same position as the intact ones, generating a smear. But the intact terminal fragments (H and I), which were generated from the termini that were not digested by exonuclease III, should maintain a constant fluorescence ratio on the gel if exonuclease III has an equal probability of digesting the two termini. The results (Fig. 8, lanes 7 to 10) indicated that the nuclease had an easier access to the I fragment, and therefore confirmed the conclusion from the previous section that the right terminus of the CELO virus DNA is on the outside of the core.

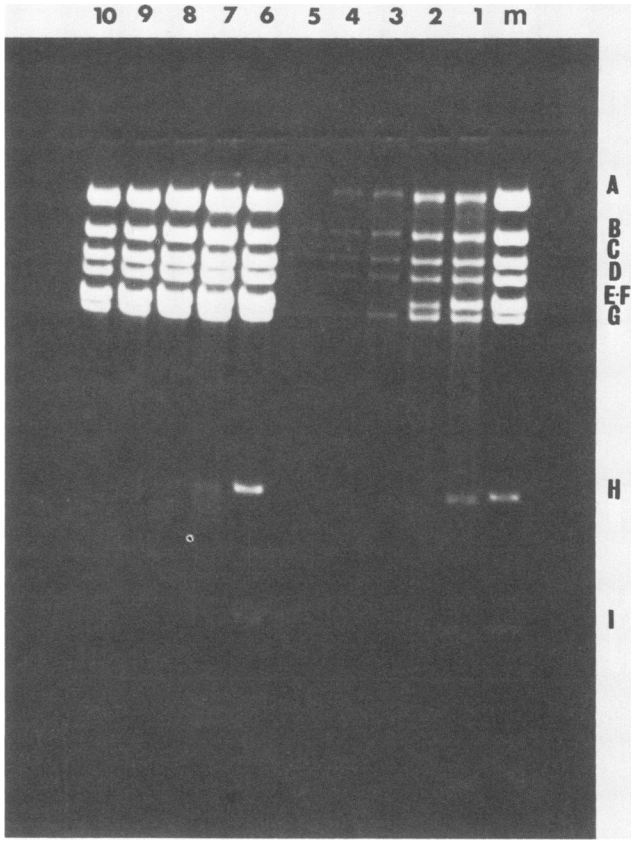

FIG. 8. *Hin*dIII restriction patterns of DNA from CELO virus cores digested with exonuclease III and Mung Bean ss-endonuclease. Purified CELO virus DNA or CELO virus cores were digested with exonuclease III and then with Mung Bean ss-specific endonuclease as specified in the text. The DNAs were then extracted, digested with *Hin*dIII, and analyzed by electrophoresis on a 1.2% agarose gel. Lane m, intact CELO virus DNA marker. Lanes 1 to 5, CELO virus DNA digested by exonuclease III for 0, 2, 5, 10, and 20 min, respectively, followed by Mung Bean ss-specific endonuclease digestion. Lanes 6 to 10, DNA from CELO virus cores digested by exonuclease III for 0, 5, 10, 20, and 40 min, respectively, followed by Mung Bean ss-specific endonuclease digestion.

DISCUSSION

We reported in this paper CELO virus cores prepared by the pyridine method contained three prominent core proteins (CELO virion polypeptides IX, XI, and XII), which are all small molecules with polypeptide molecular weights less than 20,000 present in the virion in large numbers (Li et al., in press). The smallest CELO virus core polypeptide (XII), like polypeptide VII of human adenovirus, was most tightly attached to the viral DNA, whereas the other two core polypeptides were dissociated from the DNA by Sarkosyl treatment. CELO virus polypeptide XII is present in the virion at a number roughly equal to that of Ad5 polypeptide VII in the Ad5 virion. However, the size of CELO virus polypeptide XII is only half that of Ad5 polypeptide VII. Considering that CELO virus DNA is 30% larger than its human counterpart, it presumably requires larger numbers of the other two core protein species to package the viral DNA into the core.

It is also reported in this paper that CELO virus cores prepared by the pyridine method may have a slightly more compact morphology than the Ad5 pyridine cores. Cores from both viruses appeared to consist of an electron-dense body probably containing the DNA, and a more lightly stained outer area which may consist of protein. Electron microscope and neutron scattering studies of human adenovirus cores have suggested similar conclusions (4, 10, 38). In some cases, a number of discrete subcore domains were visible in the CELO virus core (Fig. 2c′), consistent with the reported existence of 12 subcore domains in the core of human adenoviruses (4, 39a).

Experiments reported in this paper showed that micrococcal nuclease digestion of CELO virus cores did not generate a nucleosome repeat pattern of DNA fragments with 200-bp intervals. Furthermore, the micrococcal nuclease-digested fragments of CELO virus cores were shown not to behave like nucleosomes. The main evidence for the first chromatin-like model for the adenovirus core was the reported nucleosomal repeat pattern of the viral DNA generated by micrococcal nuclease digestion of the virus cores (5). However, this has not been reproduced by subsequent investigators.

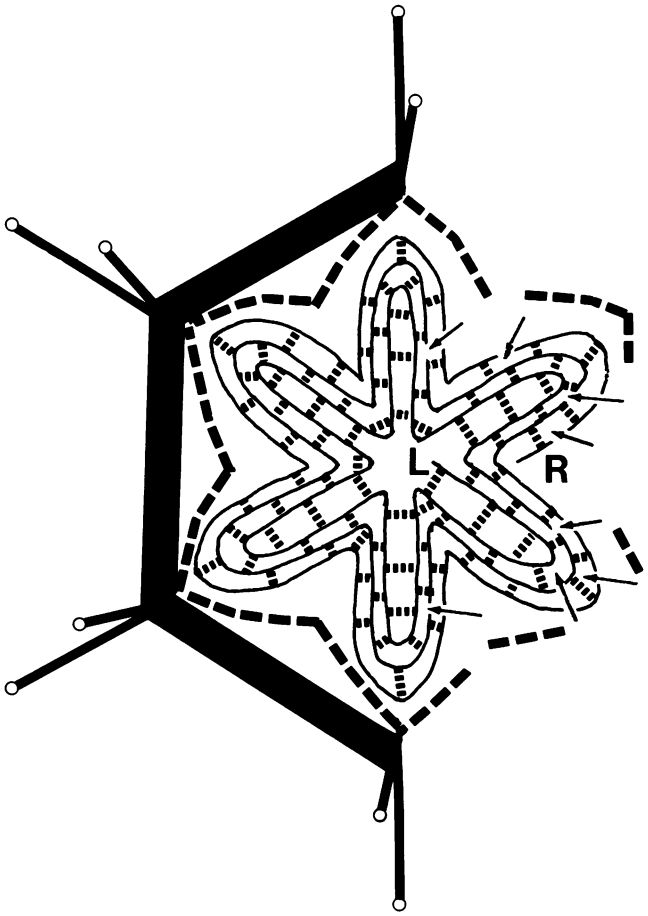

FIG. 9. Model for the structure of the avian adenovirus core. The left-hand part shows the proposed structure of an intact virion. There are two fibers carried by each penton base (31). Inside the virion capsid (represented by bold solid lines) is a thin shell made of protein(s) represented by dotted lines. Further inside is a core consisting of the DNA (fine solid line), condensed and cross-linked by core proteins. The left-hand (L) end of the DNA is located in the interior. The right-hand part of the model shows a released virus core being digested by micrococcal nuclease (represented by small arrows). The protein shell is broken. The micrococcal nuclease cuts the viral DNA into fragments that are still held by protein linkers. The right-hand (R) end of the DNA would be digested more quickly if the DNA encapsidation always started from the left end. The topology of condensation indicated may account for subcore domains, but other forms of highly condensed quasi-parallel arrays are possible (see the text) (12, 13).

The second chromatin-like model for the adenovirus core (37) was based on a nuclease-resistant 150-bp nucleosome-core structure, and the absence of an expected nucleosome repeat pattern was attributed to irregular spacing of the nucleosome-core structures along the viral DNA. The nucleosome core structure proposed would be a small and tightly organized nucleoprotein, which should be able to enter a 4% polyacrylamide gel and should be detected by both DNA-specific and protein-specific stains, as was demonstrated with micrococcal nuclease-digested chicken RBC nuclei. The negative results with CELO virus cores reported in this paper thus argue against the 150-bp nucleosome-core structure. A diffuse band in this size range has been reported when deproteinized DNA was digested with micrococcal nuclease under certain conditions (47, 57). There may be differences between human and avian adenoviruses, but the micrococcal nuclease digestion results we obtained with CELO virus cores are very similar to the majority of those published for human adenovirus cores.

The third experimental observation for the chromatin-like models was the reported "beads-on-a-string" appearance (37, 57), but the electron micrographs published appear different from those of eucaryotic chromatin (40) or papovavirus minichromosomes, which use cellular histones as their core proteins (2, 18, 20). In addition, this type of structure can be generated in DNA samples in the total absence of proteins under some conditions (13), and some of the structures observed by adenovirus investigators at high salt concentrations were found not to be nuclease resistant (57). With the main evidence reexamined, an obvious choice now is to abandon chromatin-like models for the cores of all adenoviruses.

As an alternative, it is proposed that adenovirus DNA is progressively neutralized and cross-linked by the basic core proteins, resulting in condensation into the core. Similar models have been proposed for condensation of DNA into bacteriophage heads by polyamines (1, 12, 28, 52). One type of condensation that would explain our results and the apparent existence of 12 subcore domains is shown in Fig. 9, but any type of folding or winding into quasi-parallel arrays cross-linked by core proteins would be consistent with the results. As the hydrated volume of the DNA plus core proteins is larger than the calculated volume of the core, the DNA must be highly condensed and water may be excluded. The organization into subcore domains could also be due to passive containment by an appropriately shaped protein shell between the capsid and inner core, for which there is some evidence (4, 10, 38). The protein cross-linked model is consistent with the observation that in micrococcal nuclease-digested CELO virus cores not exposed to protease, the majority of small DNA fragments do not enter a 4% acrylamide gel either as free DNA or as discrete nucleoproteins (Fig. 9, right side). The protein cross-linked model can also accomodate neutron and X-ray scattering data (10) which suggest a non-chromatin-like, yet ordered, DNA organization inside the adenovirus core.

In the chromatin-like models (5, 37), the human adenovirus major core protein (polypeptide VII) was regarded as the equivalent of the inner histones of eucaryotes (H2a, H2b, H3, and H4). Recently, Sung et al. (51) determined the DNA and amino acid sequence of Ad2 polypeptide VII. The protein contains four basic domains separated by three to four predicted α-helices. In addition, one of the four basic domains is a very basic, protamine-like domain, and two other basic domains are located at the two ends of the polypeptide. This structure thus resembles a histone H1-protamine hybrid and has little in common with the structure of the inner histones of eucaryotes. The essential structural feature of inner histones is a small basic arm at one end of the molecule connected to a globular stem at the other end of the molecule (27, 36). It was suggested that hydrophobic interactions between the globular stems of the four inner histones (3, 24) led to the formation of the protein kernel of the nucleosome core. On the other hand, the histone H1 molecule has three structural domains: two basic domains at the ends, and a globular domain in the middle of the polypeptide. This structure probably explains why histone H1 is involved in the higher order condensation of DNA in the chromatin rather than in the nucleosome core structure (26).

The histone H1-protamine hybrid structure with four basic

arms of the human adenovirus major core proteins suggests that the monomer molecules, rather than the hypothetical hexamer (37), may directly interact with DNA. The existence of the protamine-like domain also suggests a role, similar to that of protamine in the structure of nucleoprotamine, played by the major core protein. Based on studies of the structure of protamine and its interaction with tRNA, Warrant and Kim (58) proposed a nucleoprotamine model in which the protamine molecules act as a DNA condensation agent by wrapping around the major groove of the DNA double helix and cross-linking successive turns of DNA. These authors also pointed out the possibility that similar interactions might exist in the structure of other nucleoproteins. The structural features of the human adenovirus major core protein suggest that it may have a protamine-like manner of DNA condensation. Interactions between α-helices and the major groove of the double helix of DNA have recently been implicated in a number of DNA-binding proteins (53).

From a biological point of view, the protein cross-linked, highly condensed wrapped structure for the core suggests why, upon entry into infected cells, adenovirus core proteins are apparently replaced by cellular histones to form nucleosome-like structures at an early stage of infection (7, 54). In the protein cross-linked model, the replacement of adenovirus core proteins by histones early after infection can be envisaged as resembling the decondensation of the cross-linked nucleoprotamine of the sperm in the process of fertilization, as suggested by Sung et al. (51). This may explain in part the requirement for a modification of each incoming adenovirus genome before it can begin the early stage of transcription, despite the presence in the same cell of other genomes that have already commenced transcription (17).

Models of adenovirus DNA encapsidation have been based on studies of defective or incomplete particles formed by human adenovirus from subgroup A (Ad12), subgroup B (Ad3, Ad7, and Ad16), subgroup C (Ad2), and simian adenovirus SA7 (56). Such incomplete or defective particles contain less DNA than normal, but the DNA they contain enables them to retain the ability to transform rodent cells, indicating the presence of the left-hand end (46). Further analysis of the DNAs isolated from defective particles of Ad2 and Ad3 by restriction endonuclease digestion and other means has confirmed that they are rich in sequences from the left ends of the viral genomes (6, 55), whereas sequences from both ends of the genome were equally present in the pool of subgenomic DNA molecules in infected cells (8, 21). This indicates that there is a preferential packaging of sequences containing the left end of the genome. Similarly, Ginsberg also found that the partially encapsidated DNA in the heavy intermediate structure found during virion assembly is enriched in sequences homologous to the left-hand end of the viral genome (56). More detailed study has led to the identification of a packaging sequence between 290 and 390 bp from the left terminus of the genome, that directs the polar encapsidation of adenovirus DNA (21, 29). Our experiments involving digestion with micrococcal nuclease and with exonuclease III followed by Mung Bean ss-endonuclease indicated that the right-hand terminus of CELO virus DNA was on the outside of the core and the left hand was at the center, according to the orientation of CELO virus DNA suggested by Denisova et al. (9), which we have accepted in preference to that proposed by Shimada et al. (48). We therefore suggest that condensation of the DNA begins at the packaging sequence and proceeds by cross-linking and neutralization of the DNA by the core proteins, the right end being encapsidated last (Fig. 9).

ACKNOWLEDGMENTS

We thank Lesley M. Maxwell for electron microscopy, and Lydia K. Waldron-Stevens and Dianne Gallasch for technical assistance.

LITERATURE CITED

1. **Becker, A., M. Marko, and M. Gold.** 1977. Early events in the *in vitro* packaging of bacteriophage DNA. Virology **78**:291–305.
2. **Bellard, M., P. Oudet, J. E. Germond, and P. Chambon.** 1976. Subunit structure of simian-virus-40 minichromosome. Eur. J. Biochem. **70**:543–553.
3. **Bradbury, E. M., T. Moss, H. Hayashi, R. P. Hjelm, P. Suan, R. M. Stephens, J. P. Baldwin, and C. Crane-Robinson.** 1977. Nucleosomes, histone interactions and the role of histones H3 and H4. Cold Spring Harbor Symp. Quant. Biol. **42**:277–286.
4. **Brown, D. T., M. Westphal, B. T. Burlingham, U. Winterhoff, and W. Doerfler.** 1975. Structure and composition of the adenovirus type 2 core. J. Virol. **16**:366–387.
5. **Corden, J., M. H. Engelking, and G. Pearson.** 1976. Chromatin-like organization of the adenovirus chromosome. Proc. Natl. Acad. Sci. U.S.A. **73**:401–404.
6. **Daniell, E.** 1976. Genomic structure of incomplete particles of adenovirus. J. Virol. **19**:685–708.
7. **Daniell, E., D. E. Groff, and M. J. Fedor.** 1981. Adenovirus chromatin structure at different stages of infection. Mol. Cell Biol. **1**:1094–1105.
8. **Daniell, E., and T. Mullenbach.** 1978. Synthesis of defective viral DNA in HeLa cells infected with adenovirus type 3. J. Virol. **26**:61–70.
9. **Denisova, T. S., B. S. Sitnikov, and R. A. Ghibadulin.** 1979. Study of DNA fragmentation of chick adenovirus CELO by specific endonucleases R.HpaI, R.EcoRI, R.HindIII. Mol. Biol. (Moscow) **13**:1021–1034.
10. **Devaux, C., P. A. Timmins, and C. Berthet-Colominas.** 1983. Structural studies of adenovirus type 2 by neutron and x-ray scattering. J. Mol. Biol. **167**:119–132.
11. **Doerfler, W., and A. K. Kleinschmidt.** 1970. Denaturation pattern of the DNA of adenovirus 2 as determined by electron microscopy. J. Mol. Biol. **50**:579–593.
12. **Earnshaw, W. C., and S. C. Harrison.** 1977. DNA arrangement in isometric phage heads. Nature (London) **268**:598–602.
13. **Eickbush, T. H., and E. N. Moudrianakis.** 1978. The compaction of DNA helices into either continuous supercoils or folded-fiber rods and toroids. Cell **13**:295–306.
14. **Everitt, E., L. Lutter, and L. Philipson.** 1975. Structural proteins of adenoviruses. XII. Location and neighbour relationship among proteins of adenovirion type 2 as revealed by enzymatic iodination, immunoprecipitation and chemical cross-linking. Virology **67**:197–208.
15. **Everitt, E., B. Sundquist, U. Pettersson, and L. Philipson.** 1973. Structural proteins of adenoviruses. X. Isolation and topography of low molecular weight antigens from the virion of adenovirus type 2. Virology **52**:130–147.
16. **Fedor, M. J., and E. Daniell.** 1983. DNAse I cleavage of adenovirus nucleoprotein. Nucleic Acids Res. **11**:4417–4434.
17. **Gaynor, R. B., and A. J. Berk.** 1983. *cis*-acting induction of adenovirus transcription. Cell **33**:683–693.
18. **Germond, J. E., B. Hirt, P. Oudet, M. Gross-Bellard, and P. Chambon.** 1975. Folding of the DNA double helix in chromatin-like structures from simian virus 40. Proc. Natl. Acad. Sci. U.S.A. **72**:1843–1847.
19. **Goodwin, G. H., and A. E. Dahlberg.** 1982. Electrophoresis of nucleoproteins, p. 199–210. *In* D. Rickwood, and B. D. Hames (ed.), Gel electrophoresis of nucleic acids. IRL Press Ltd., Oxford.
20. **Griffith, J. D.** 1975. Chromatin structure: deduced from a minichromosome. Science **187**:1202–1203.
21. **Hammarskjold, M. L., and G. Winberg.** 1980. Encapsidation of adenovirus 16 DNA is directed by a small DNA sequence at the left end of the genome. Cell **20**:787–795.

22. **Hayat, M. A.** 1981. Principles and techniques of electron microscopy. Biological applications, vol. 1, 2nd ed., p. 327–337. University Park Press, Baltimore, Md.
23. **Hewish, D. R., and L. A. Burgoyne.** 1973. Chromatin substructure: the digestion of chromatin DNA at regular spaced sites by a nuclear deoxyribonuclease. Biochem. Biophys. Res. Commun. **52**:504–510.
24. **Hörz, W., and H. G. Zachau.** 1980. Deoxyribonuclease II as a probe for chromatin structure. I. Location of cleavage sites. J. Mol. Biol. **144**:305–327.
25. **Hosokawa, K., and M. T. Sung.** 1976. Isolation and characterization of an extremely basic protein from adenovirus type 5. J. Virol. **17**:924–934.
26. **Igo-Kemenes, T., W. Hörz, and H. G. Zachau.** 1982. Chromatin. Annu. Rev. Biochem. **51**:89–121.
27. **Isenberg, I.** 1979. Histones. Annu. Rev. Biochem. **48**:159–191.
28. **Kaiser, D., M. Syvanen, and T. Masuda.** 1975. DNA packaging steps in bacteriophage lambda head assembly. J. Mol. Biol. **91**:175–186.
29. **Kosturko, L. D., S. V. Sharnick, and C. Tibbetts.** 1982. Polar encapsidation of adenovirus DNA: cloning and DNA sequence of the left end of adenovirus type 3. J. Virol. **43**:1132–1137.
30. **Laemmli, U. K.** 1970. Cleavage of structural proteins during the assembly of the head of bacteriophage T4. Nature (London) **227**:680–685.
31. **Laver, W. G., B. H. Younghusband, and N. G. Wrigley.** 1971. Purification and properties of chick embryo lethal orphan virus (an avian adenovirus). Virology **45**:598–614.
32. **Li, P., A. J. D. Bellett, and C. R. Parish.** 1983. A comparison of the terminal protein and hexon polypeptides of avian and human adenoviruses. J. Gen. Virol. **64**:1375–1379.
33. **Lonberg-Holm, K., and L. Philipson.** 1969. Early events of virus-cell interaction in an adenovirus system. J. Virol. **4**:323–338.
34. **Maniatis, T., E. F. Fritsch, and J. Sambrook.** 1982. Molecular cloning, a laboratory manual. Cold Spring Harbor Laboratory, Cold Spring Harbor, N.Y.
35. **Marx, K. A., and T. C. Reynolds.** 1982. Spermidine-condensed ϕX174 DNA cleavage by micrococcal nuclease: torus cleavage model and evidence for unidirectional circumferential DNA wrapping. Proc. Natl. Acad. Sci. U.S.A. **79**:6484–6488.
36. **McGhee, J. D., and G. Felsenfeld.** 1980. Nucleosome structure. Annu. Rev. Biochem. **49**:1115–1156.
37. **Mirza, M. A., and J. Weber.** 1982. Structure of adenovirus chromatin. Biochim. Biophys. Acta **696**:76–86.
38. **Nermut, M. V.** 1979. Structural elements in adenovirus cores. Evidence for a "core shell" and linear structures in "relaxed" cores. Arch. Virol. **62**:101–116.
39. **Nermut, M. V.** 1980. The architecture of adenoviruses: recent views and problems. Arch. Virol. **64**:175–196.
39a. **Newcomb, W. W., J. W. Boring, and J. C. Brown.** 1984. Ion etching of human adenovirus 2: structure of the core. J. Virol. **51**:52–56.
40. **Olins, D. E., and A. L. Olins.** 1974. Spheroid chromatin units (υ bodies). Science **183**:330–332.
41. **Prage, L., U. Pettersson, S. Hoglund, K. Lonberg-Holm, and L. Philipson.** 1970. Structural proteins of adenoviruses. IV. Sequential degradation of the adenovirus type 2 virion. Virology **42**:341–358.
42. **Roberts, W. K., C. A. Dekker, G. W. Rushisky, and C. A. Knight.** 1962. Studies on the mechanism of action of micrococcal nuclease. I. Degradation of the thymus deoxyribonucleic acid. Biochim. Biophys. Acta **55**:664–673.
43. **Robinson, A. J., and A. J. D. Bellett.** 1974. A circular DNA-protein complex from adenoviruses and its possible role in DNA replication. Cold Spring Harbor Symp. Quant. Biol. **39**:523–531.
44. **Robinson, A. J., H. B. Younghusband, and A. J. D. Bellett.** 1973. A circular DNA-protein complex from adenoviruses. Virology **56**:54–69.
45. **Rylatt, D. B., and C. R. Parish.** 1982. Protein determination on an automatic spectrophotometer. Anal. Biochem. **121**:213–214.
46. **Schaller, J. P., and D. S. Yohn.** 1974. Transformation potentials of the noninfectious (defective) component in pools of adenoviruses type 12 and simian adenovirus 7. J. Virol. **14**:392–401.
47. **Sergeant, A., M. A. Tigges, and H. J. Raskas.** 1979. Nucleosome-like structural subunits of intranuclear parental adenovirus type 2 DNA. J. Virol. **29**:888–898.
48. **Shimada, K., T. Yoshida, T. Kuroishi, and M. Ishibashi.** 1983. Restriction map of CELO virus DNA. Biochem. Biophys. Acta **740**:169–178.
49. **Southern, E.** 1980. Gel electrophoresis of restriction fragments. Methods Enzymol. **68**:152–176.
50. **Steck, G., P. Leuthard, and R. R. Burk.** 1980. Detection of basic proteins and low molecular weight peptides in polyacrylamide gels by formaldehyde fixation. Anal. Biochem. **107**:21–24.
51. **Sung, M., T. M. Cao, R. Coleman, and K. Budelier.** 1983. Gene and protein sequences of adenovirus protein VII, a hybrid basic chromosomal protein. Proc. Natl. Acad. Sci. U.S.A. **80**:2902–2906.
52. **Syvanen, M., and J. Yin.** 1978. Studies of DNA packaging into the heads of bacteriophage lambda. J. Mol. Biol. **126**:333–346.
53. **Takeda, Y., D. H. Ohlendorf, W. F. Anderson, and B. W. Matthews.** 1983. DNA-binding proteins. Science **221**:1020–1026.
54. **Tate, V. E., and L. Philipson.** 1979. Parental adenovirus DNA accumulates in nucleosome-like structures in infected cells. Nucleic Acids Res. **6**:2769–2785.
55. **Tibbetts, C.** 1977. Viral DNA sequences from incomplete particles of human adenovirus type 7. Cell **12**:243–249.
56. **Tooze, J. (ed.).** 1980. DNA tumor viruses. Molecular biology of tumor viruses, part II. Cold Spring Harbor Laboratory, Cold Spring Harbor, N.Y.
57. **Vayda, M. E., A. E. Rogers, and S. J. Flint.** 1983. The structure of nucleoprotein cores released from adenovirions. Nucleic Acids Res. **11**:441–460.
58. **Warrant, R. W., and S. H. Kim.** 1978. α-Helix-double helix interaction shown in the structure of a protamine-transfer RNA complex and a nucleoprotamine model. Nature (London) **271**:130–135.
59. **Wray, W., T. Boulika, V. P. Wray, and R. Hancock.** 1981. Silver staining of proteins in polyacrylamide gels. Anal. Biochem. **118**:197–203.
60. **Yasue, H., and M. Ishibashi.** 1977. Chick embryo lethal orphan (CELO) virus induced early and late polypeptides. Virology **78**:216–233.
61. **Younghusband, H. B., and A. J. D. Bellett.** 1971. Mature form of the deoxyribonucleic acid from chick embryo lethal orphan virus. J. Virol. **8**:265–274.
62. **Younghusband, H. B., and A. J. D. Bellett.** 1972. Denaturation pattern of the deoxyribonucleic acid from chicken embryo lethal orphan virus. J. Virol. **10**:855–857.